CONTINUOUS WAVELET TRANSFORM TECHNIQUE FOR LOW-STRAIN INTEGRITY TESTING OF DEEP DRILLED SHAFTS

Sheng-Huoo Ni [1], William M. Isenhower [2], and Yang-Hong Huang [3]

ABSTRACT

Non-destructive evaluation techniques have been adopted to provide pile construction quality control for many years. In particular, low strain pile integrity test methods have been used to check lengths and integrity of newly installed pile. The pile integrity testing signals acquired from the receivers on pile heads are complicated by defects and undesired background noise. The continuous wavelet transform (CWT) method with time-frequency distribution is adopted to enhance the characteristics of the testing signal to raise the identification ability in experimental cases. The in-situ tests of drilled shaft indicate that testing signals could be displayed in the time-frequency domain at the same time and then be explored at every single time by CWT. CWT can enhance the signal and make more information visible. Coupling CWT and Sonic Echo (SE) methods to interpret and identify the pile integrity visually, easily and quickly is proven, even for long drilled shafts.

Key words: Pile, non-destructive test, wavelet transform, sonic echo test.

1. INTRODUCTION

The drilled shaft inspector has the primary responsibility for checking the quality of the completed drilled shaft during construction. The inspector may also employ various types of non-destructive tests (NDT) to assess the quality of concrete in the shaft at the end of construction. Use of NDT methods to evaluate the integrity of drilled shafts is gaining popularity due to their advantages of low cost and rapid testing when compared to full-scale load testing (Lin *et al*. 2007). Two popular types of NDT is the crosshole sonic logging (CSL) test and various types of stress wave reflection techniques (*e.g.*, sonic echo and impulse response methods).

A reliable NDT method that can be performed at the top of the completed drilled shaft and does not require installation of access tubes might be used in situations where doubts about the quality of a shaft exist and would not need to be pre-planned. In particular, low strain pile integrity test methods (*e.g.*, sonic echo and impulse response methods) have been used to check lengths and integrity of newly installed foundations (Olson and Wright 1989). These methods can help engineers to detect and identify the presence and location of pile defects. The term "low-strain integrity testing" is derived from the fact that the device generates only low-strain stress waves in the pile. However, in practice, the signals are not always pure and without noise. The shortcoming of conventional pulse sonic echo (SE) and impulse response (IR) tests is that the results are one-dimensional; measuring only the depth of the defect below the top of shaft. Also, the tests are insensitive to defects smaller than about one half of the shaft diameter. Another shortcoming of these tests is that the shape of the shaft cannot be inferred from the test results. Additionally, conventional stress wave reflection methods are reliable in drilled shafts with embedded lengths less than 18 to 21 m, but are unreliable for longer shafts because of problems in signal measurement and processing.

A new numerical signal process tool that can improve and strengthen the signal characteristics substantially is necessary. One new method is the wavelet transform method (WTM). This signal processing technique is improved significantly by acquiring and processing lower frequency signals from the deeper portions of the drilled shaft and by using wavelet transform techniques in signal processing. The wavelet transform technique has been applied to a wide variety of signal analyses.

The wavelet transform application for low-strain integrity testing was first researched at Napier University, Edinburgh (Addison and Watson 1997; Addison *et al*. 2002). In Addison *et al*. (1997), the authors present finite element generated responses for an imaginary pile 10m in length, with and without a 20% impedance increase at mid-length. They indicate that the 20% impedance change is difficult to spot in the time domain, whereas the defect can be observed clearly in the wavelet transform (Seidel 2000). The WTM allows the signal to be decomposed so that frequency characteristics, as defined by analyzing the wavelet, and the position of particular features in a time series may be highlighted. The advantage of wavelet based signal analysis methods over traditional Fourier transform method lies in its capability to produce simultaneous temporal and scale information (Ni *et al*. 2007). However, this is the limitation for the pile integrity testing results from the necking area. The reflection shape of the wave propagated can only be identified well if the defect necking area ratio is more than over 10% in the laboratory experimental study (Hartung *et al*. 1992).

Manuscript received November 16, 2012; revised December 30, 2012; accepted December 31, 2012.

[1] Professor (corresponding author), Professor, Dept. of Civil Engineering, National Cheng Kung University, 70101, Tainan, Taiwan (e-mail: tonyni@mail.ncku.edu.tw).

[2] P.E, M. ASCE, Project Manager, Ensoft Inc., 3003 Howard Lane, Austin, Texas, 78728, USA.

[3] Engineer, Trinity Foundation Engineering Consultants Co., Ltd., Taipei, Taiwan.

This paper discusses how the continuous wavelet transform method (CWT) can be used to evaluate the characteristics of the test signal to identify in abnormalities in the concrete and the shape of the completed drilled shaft. This paper will present experimental results from field tests that indicate that the CWT method has improved the capability of processing the low-frequency signals significantly. The CWT test results from a 53 m long, 1.5 m diameter drilled shaft will also be presented in this paper.

2. WAVELET TRANSFORM METHOD

2.1 Wavelet Transform Versus Fourier Transform

Fourier transform breaks down a signal into the constituent sinusoids with different frequencies. Another point of view about Fourier analysis is view it as a mathematical technique for transforming signal to from a time-based to a frequency-based. However, the Fourier analysis has a serious drawback. When transforming a signal to the frequency domain, time information disappears. When inspecting a Fourier transformed signal, it is almost impossible to tell whether a particular event took place or not. As for the most characteristics such as abrupt changes, the beginning and the end of events, Fourier analysis obviously can not detect them at all.

In order to correct this deficiency, Gabor (1946) adapted a technique called windowing the signal (or the Short Time Fourier Transform, STFT), maps a signal into a two-dimensional function of time and frequency. The STFT represents a sort of compromise between the time and frequency-based view of signal. It provides some information about both when and at what frequencies a signal event occurs. However, it can offer this information with limited precision, and precision only is determined by the size of the window. The drawbacks of STFT are that once you choose a particular size for the time window, that window is the same for all frequencies. Many signals required a more flexible approach where we can vary the window size to determine more accurately for either time or frequency presentations.

One major advantage afforded by wavelet transform is the capability to perform local analysis, *i.e.*, to analyze a localized piece of a long duration signal. Wavelet analysis allows the choice of a long time intervals where we need more precise low-frequency information, and shorter ones where high-frequency information is needed. It is a windowing technique with variable-sized regions. Wavelet analysis is the breaking up of a signal into shifted and scaled versions of the original (or mother) wavelet, so that local features can be described better with wavelets that are concentrated on a localized region.

The WTM has been found particularly useful for analyses signals of which can be described as a periodic, noisy, intermittent, and transient. There are many different wavelet transforms available, *i.e.*, it is not a unique function. A wavelet must satisfy three conditions:

1. It must have unit energy.
2. It must provide compact support or sufficiently fast decay so that it satisfies the requirement of space (or time) location.
3. It must have zero mean, that is the integral of the wavelet function from $-\infty$ to $+\infty$ is zero. This requirement is called the admissibility condition, and it ensures that there are both positive and negative components to the mother wavelet.

2.2 Continuous Wavelet Transform

Consider a real or complex-value continuous-time function $\psi(t)$ with the following property (Daubechies 1992; Morlet 1984):

1. The function integrates to zero:

$$\int_{-\infty}^{\infty} \psi(t)\, \mathrm{d}t = 0 \tag{1}$$

2. Any square integral function, or, equivalent, has finite energy:

$$\int_{-\infty}^{\infty} |\, f(t)\,|^2\, \mathrm{d}t < \infty \tag{2}$$

The function $\psi(t)$ is a mother wavelet or wavelet if it satisfies these two properties as well as the admissibility condition as defined above. Let $f(t)$ be any square integral function. The Continuous Wavelet Transform (CWT) with respect to a wavelet $\psi(t)$ is defined as

$$W(a, b) = \frac{1}{\sqrt{a}} \int_{-\infty}^{+\infty} f(t)\psi^* \left(\frac{t-b}{a} \right) \mathrm{d}t \tag{3}$$

where a and b are real and $*$ denotes the complex conjugate. We set $\psi_{a,b}(t)$ as

$$\psi_{a,b}(t) = \frac{1}{\sqrt{|\,a\,|}} \psi^* \left(\frac{t-b}{a} \right) \tag{4}$$

Then, combining Eqs. (3) and (4), yields

$$W(a, b) = \int_{-\infty}^{+\infty} f(t)\psi_{a,b}(t)\, \mathrm{d}t \tag{5}$$

The variable b represents the time shift or translation, and variable a determines the amount of time scaling or dilation. Since the CWT is generated using dilates and translates of the signal function $\psi(t)$, the wavelet for the transform is referred to as the mother wavelet. Next we generate a set of expansion functions so that any signal in $L^2(\mathrm{R})$ (the space of squared integral functions) can be represented by the series

$$f(t) = \sum_{j,k} a_{j,k} \sqrt{2^j}\, \varphi\, (2^j t - k) \tag{6}$$

when we set

$$\psi(t) = \sum_{n} h(n) \sqrt{2} \varphi(2t - n)\,, \quad n \in Z \tag{7}$$

where coefficients $h(n)$ are a sequence of real or perhaps complex numbers called the scaling function coefficients and the $\sqrt{2}$ maintains the norm of the scaling function with the scale two. The function generated by Eq. (7) gives the prototype or mother $\varphi(t)$ for a class of expansion functions of the form k,

$$\psi_{j,k}(t) = 2^{\frac{j}{2}} \psi\, (2^j\, t - k) \quad \forall j, k \in Z \tag{8}$$

We constructed a set of functions $\psi(t)$ and $\psi_{j,k}(t)$ that could span all of L^2 (R). Any signal function $f(t) \in$ R could be written as

$$f(t) = \sum_{k=-\infty}^{+\infty} c(k)\, \varphi_k(t) + \sum_{j=0}^{\infty} \sum_{k=-\infty}^{+\infty} d(j,k)\, \psi_{j,k}(t) \tag{9}$$

A more general statement of the expansion can be written as

$$f(t) = \sum_{k} c_{jo}(k) \varphi_{j_0,k}(t) + \sum_{k} \sum_{j=j_0}^{\infty} d_j(k)\, \psi_{j,k}(t) \tag{10}$$

It's a series expansion in terms of the scaling function and wavelets. In Eq. (10), the first summation gives a function that is of a low resolution or coarse approximation of $f(t)$. For each index j in the second summation, a higher or fine resolution function is added which increase more details.

The continuous wavelet transform is the sum over all time of the signal multiplied by scaled, shifted versions of the wavelet. This process produces wavelet coefficients that are a function of scale and position. In fact, here are the procedures for creating a CWT (Ni and Lo 2006):

1. Take a wavelet and compare it to a section at the start of the original signal.
2. Calculate a number, coefficient C, that represents how closely correlated the wavelet is with this section of the signal. The higher *C* is, the more the similarity. More precisely, if the signal energy and the wavelet energy are equal to one, *C* may be interpreted as a correlation coefficient. But the results will depend on the shape of the wavelet mother function chosen.
3. Shift the wavelet to the right and repeat above procedures until the whole signal have been covered.
4. Scale (stretch) the wavelet and repeat steps 1 through 3.
5. Repeat steps 1 through 4 for all scales.

When these procedures are done, the coefficients would produce at different scales by different sections of the signal. The coefficients constitute the results of a regression of the original signal performed on the wavelets. A 3D plot could be made on which the *x*-axis represents position along the signal (time), the *y*-axis represents scale, and the color or *z*-axis at each *x*-*y* point represents the magnitude of the wavelet coefficient *C*.

Besides, as with the Fourier transform, the original signal may be reconstructed:

$$f(t) = \frac{1}{C_g} \int_{-\infty}^{+\infty} \int_{-\infty}^{+\infty} \frac{1}{\sqrt{a}} \psi\left(\frac{t-b}{a}\right) W(a,b) \frac{\mathrm{d}a\mathrm{d}b}{a^2} \tag{11}$$

where C_g is the admissibility constant;

$$C_g = \int_0^{\omega} \frac{|\hat{\psi}(\omega)|^2}{\omega} \mathrm{d}\omega \tag{12}$$

where $\hat{\psi}(\omega)$ is the continuous-time function $\psi(t)$ in frequency domain, ω is the angular frequency. As the wavelet transform given by Eq. (3) is a convolution of the signal with a wavelet function, we can use the convolution theorem to express the integral as a product in Fourier space, *i.e.*,

$$W(a,b) = \frac{1}{2\pi} \int_{-\infty}^{\infty} \hat{f}(\omega)\, \hat{\psi}^*_{a,b}(\omega)\, \mathrm{d}\omega \tag{13}$$

where $\hat{\psi}^*_{a,b}(\omega) = \sqrt{a}\ \hat{\psi}^*(a\omega)\, e^{i\omega b}$

This is the Fourier spectrum of the analyzed wavelet at scale *a* and location *b*. In this way, a fast Fourier transform (FFT) algorithm can be employed in practice to compute the wavelet transform. For more details of the wavelet with time-frequency, refer to Waston and Addison (2002). A similar 3D plot then could be made on which the *x*-axis represents position along the signal (time), the *y*-axis represents frequency, and the color or *z*-axis at each *x*-*y* point represents the magnitude of the wavelet coefficient.

2.3 Morlet Mother Wavelet

To apply the CWT in any application, it is important to select the most appropriate (or optimal) mother wavelet function for the analysis. The selection is usually done by trial and error, and other wavelet forms are possible, each having particular strengths and drawbacks. In general, there is a trade-off between spatial and spectral resolution inherent in the choice of wavelet, and this function is popular in vision analysis. In this paper, we are interested in the relatively higher frequency content of the signal. As it will show that the signals contain the information necessary to detect the defect in the structure. The main idea behind the use of wavelets for structure identification purposes is based on the fact that the presence of defects introduces small discontinuities in the structure response at the damaged sites. Often these discontinuities cannot be observed from the examination of the structure response in the time domain or the frequency domain, but they are detectable from the distribution of the wavelet coefficients (or amplitude) obtained from the CWT.

The truncated Morlet wavelet function, as shown in Fig. 1, is given by (MathWorks 1996):

$$\psi(t) = e^{-\frac{t^2}{2}} \cos 5t \tag{14}$$

The function is popular in vision analysis, where it was also christened. But the scale functions φ do not exist, the analysis is not orthogonal and thus the DWT are unavailable.

3. PILE INTEGRITY TEST

The pile integrity test (PIT) helps the user to judge the integrity of each pile that major discontinuities or defects may exist, as shown in Fig. 2. For a quick and reliable assessment of the quality of a pile, graphs of velocity-time are presented together for the whole duration of a SE test. In a pile integrity test, the pile head is struck with a small hand held hammer while the pile head movement is recorded using an accelerometer or velocity transducer. The hammer blow generates a compression wave in the pile and that reflects from pile tip and any defects that might be present. Both the stress wave inputs and the reflections are measured as a function of time by an accelerometer attached to the top of pile and the acceleration spectra is integrated to obtain the velocity spectra.

The wavelet transform allows decomposition of the response signal while retaining the temporal information. The pile length *L* can be calculated from the sample number by

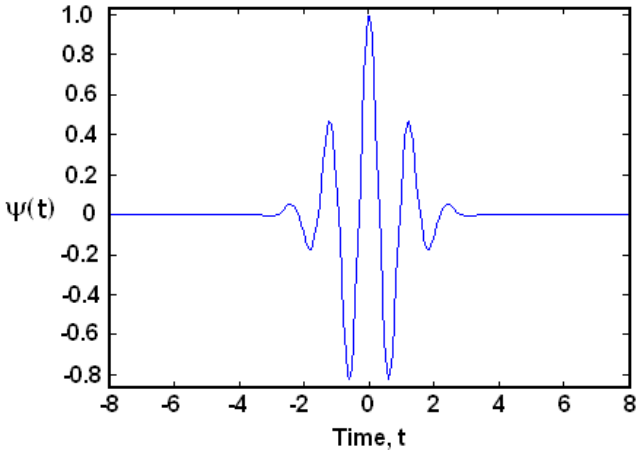

Fig. 1 Display of Morlet wavelet function

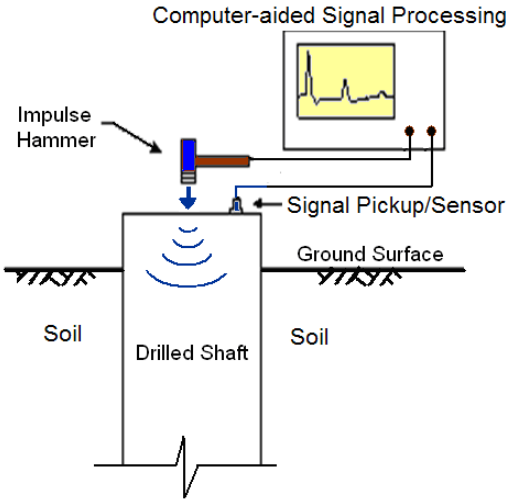

Fig. 2 Schematic drawing of pile integrity test

$$L = \frac{c / f \times \text{Sample No.}}{2} \tag{15}$$

here c is the compression wave velocity of pile and f is the sampling frequency.

The analysis is carried out using complete Morlet wavelets on the sonic echo data. For the initial tests conducted, some test piles were partly intact, others have defects, and the depth of the pile tip is of specific interest. The location of the tip is found by analyzing the signal echo reflection from the interface between the tip of the pile and the surrounding earth. The depth of the tip can then be calculated by knowing the speed of the propagation of the stress wave through the pile material (normally assumed to be 4,000 m/sec). These signals contain obvious components of reflection characteristics: (1) initial pulse of pile head; (2) reflection pulse of pile tip and (3) defects, if they exist.

4. TESTING EQUIPMENT

To obtain a high quality signal for the in-situ sonic echo test, an optimal configuration of the hammer force source, sensor and signal capture facility are needed. A typical set of equipment is shown in Fig. 3. The equipment consists of a calibrated impulse hammer, geophone sensors, and a computer-controlled signal capturer (signal analyzer).

1. Impacting Force — The optimum impact force resolution is limited by the geometry of the pile shape, and it is an important factor in the signal quality, too. In this study, a handheld impulse hammer, as shown in Fig. 3, with a weight of 5.5 kgf (12 lbf), which is made by PCB Piezotronics, Inc., USA, is used to create the pulse source. Four plastic head with different stiffness can be used to be attached to the hammer to create the different frequency contents of the impulse wave. A typical time history curve of hand held hammer impact on pile head is recorded as shown in Fig. 4(a), which shows the loading duration is about 0.7 msec. Then this signal can be transformed to frequency domain by Fast Fourier Transform (FFT) as shown in Fig. 4(b), the signal frequency bandwidth is 0 ~ 2500 Hz.
2. Geophone — Seismic velocity pickups is used as the geophone for detecting the seismic signal. The geophone of model L28B is made by Mark Products, USA. The resonant frequency of the geophone is 4.5 Hz.
3. Signal Capturer — Computer-aided Spectrum Analyzer (Model HP35650A). The measuring hardware combined with the application software and a host computer forms a high performance multi-channel signal capturing and signal processing system. The hardware acquires signals both in time and frequency domains and is capable of being configured easily for large amount of multiple input, multiple output measurements. System characteristics include: Signal acquisition and processing up to 102.4 kHz, host-independent-interfaces to any computer that supports the IEEE-488 interface, 102.4 kHz real-time bandwidth, and display updates of 64 spectra /sec. The recording mechanism is controlled by the impact loading. When the load cell within the hammer is triggered, then the geophone starts to record the particle vibration of the pile head.

5. TESTING AND RESULTS

5.1 Experimental Test

Before the experimental test, the numerical case studies had proved the feasibility of the SE method with CWT time-frequency analysis (Ni *et al*. 2006). Figures 6 ~ 7 show the intact pile and pile with defect at full scale, which have been tested in situ. These two precast concrete (PC) piles are 6 m in length and 0.3 m in diameter. The defective pile is attached as a necking area on a one side between 3.7 m and 4 m below the pile head as shown in Fig. 5. The resulting time history curve and CWT plots are shown in Fig. 6. The ideal SE test result is shown at the top graph of Fig. 6. The pile head could be localized about 0.4 msec and tip location about 3.3 msec. There are clear characters of the pile head and tip at the same position as in time domain. In addition, the main frequency bandwidth of the whole signal exists at 1.2 kHz. The frequency content maintains the same amplitude at the pile head and decays from the lower frequency 1.2 kHz to the higher one 2 kHz at the pile tip.

The results of testing of a pile with necking in the time domain and the wavelet domain graph is shown in Fig. 7. Obviously, besides both pile head and tip, there is a distinct signal character that occurred at about 2 msec. The frequency bandwidth of the defect is extended from 1.2 kHz to 1.6 kHz, and the

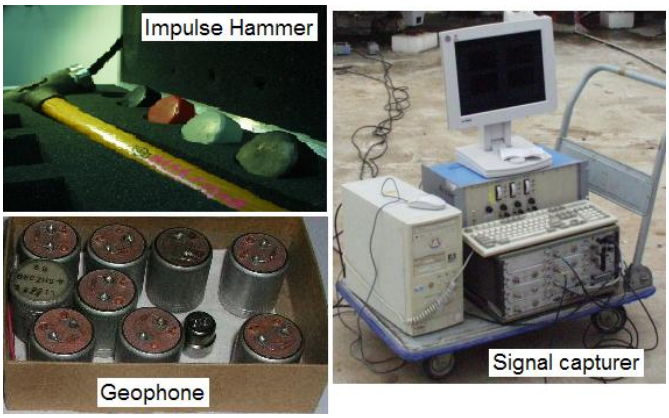

Fig. 3 Test equipment

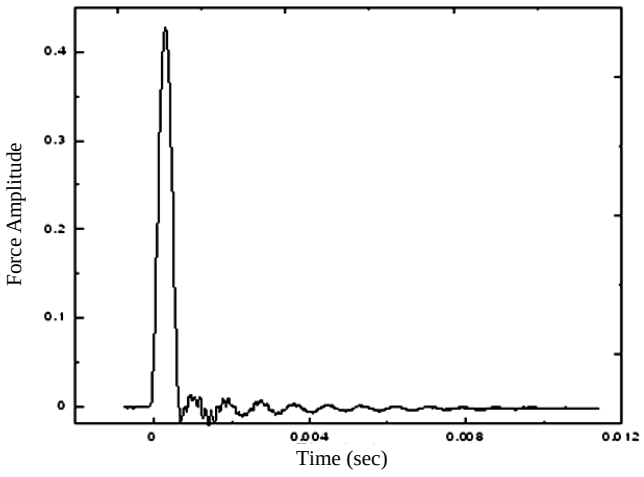

(a)

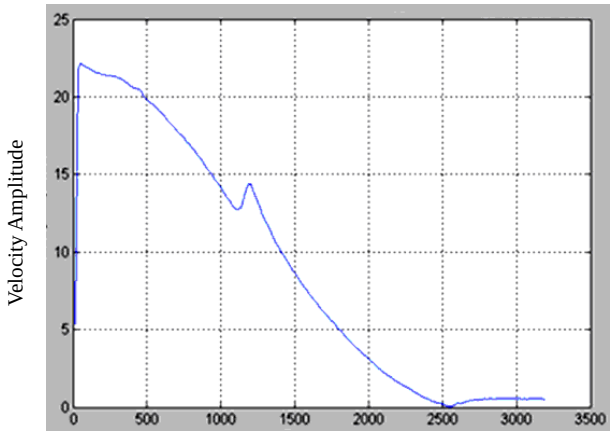

(b)

Fig. 4 (a) Impact force time history curve; (b) Impact force spectrum of a PC pile integrity test by hand held hammer impact force

amplitude gradually decayed. In summary, we could obtain the same results in the pile integrity evaluation both in the time or wavelet domain. Anyone can identify the signal characteristics visually without requiring professional knowledge of wave propagation theory, and thus we can avoid misjudging the data by interpretation of a confused and unclear signal. These two cases also prove that (1) the defect and lower end of a pile could be detected and identified clearly and accurately by coupling the SE and wavelet time-frequency analyses, and (2) the whole signal frequency contents could be realized at every single time including the defect.

5.2 In-Situ Test of Drilled Shafts

A test site located at southern Taiwan was selected to perform sonic echo test and analyzed with WTM. The pile foundation is constructed as a bridge foundation. The size of pile cap is 25.5 m by 29.25 m and located at 17 m below ground surface. The layout of piles under pile cap is shown in Fig. 8. As shown in the figure, a total of 56 piles support the foundation. Each pile is designed as 53 m long with diameter of 1.5 m, and it is constructed using fully casing drilled shaft method. Figures 9 and 10 shows the test site and drilled shafts constructed. The purpose of sonic echo test of pile is to evaluate the length of drilled shafts and to inspect the integrity of piles. The top of each pile is cleaned and geophone is fixed at the top of pile using hydro- stone before the testing. Testing is performing as shown in Fig. 11. Usually, each pile is hit about three times. All measured responses of the geophone are stored in the computer. The signals are then analyzed using WTM. A typical result is shown in Fig. 12. The upper part graph in Fig. 12 is time domain data obtained from SE test. The lower part graph in Fig. 12 is analyzed using CWT at the fourth level. The analytical program is coded using Matlab with CWT tools. In the figure it is easy to see the signal reflected from the end of pile after the CWT analysis. It took about one day to finish the testing of 56 piles.

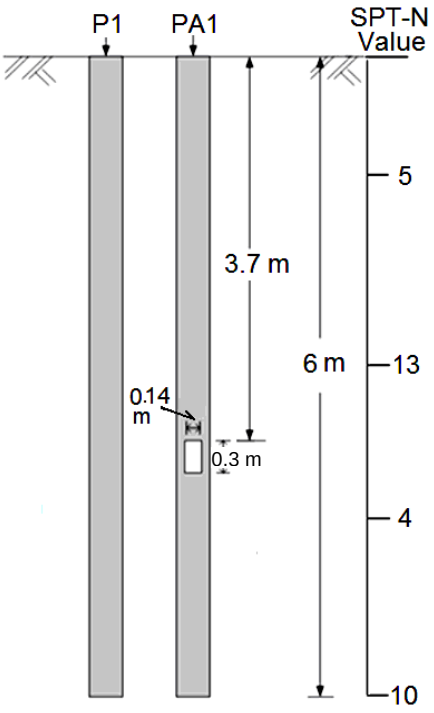

Fig. 5 Two tested model piles with soil surrounded

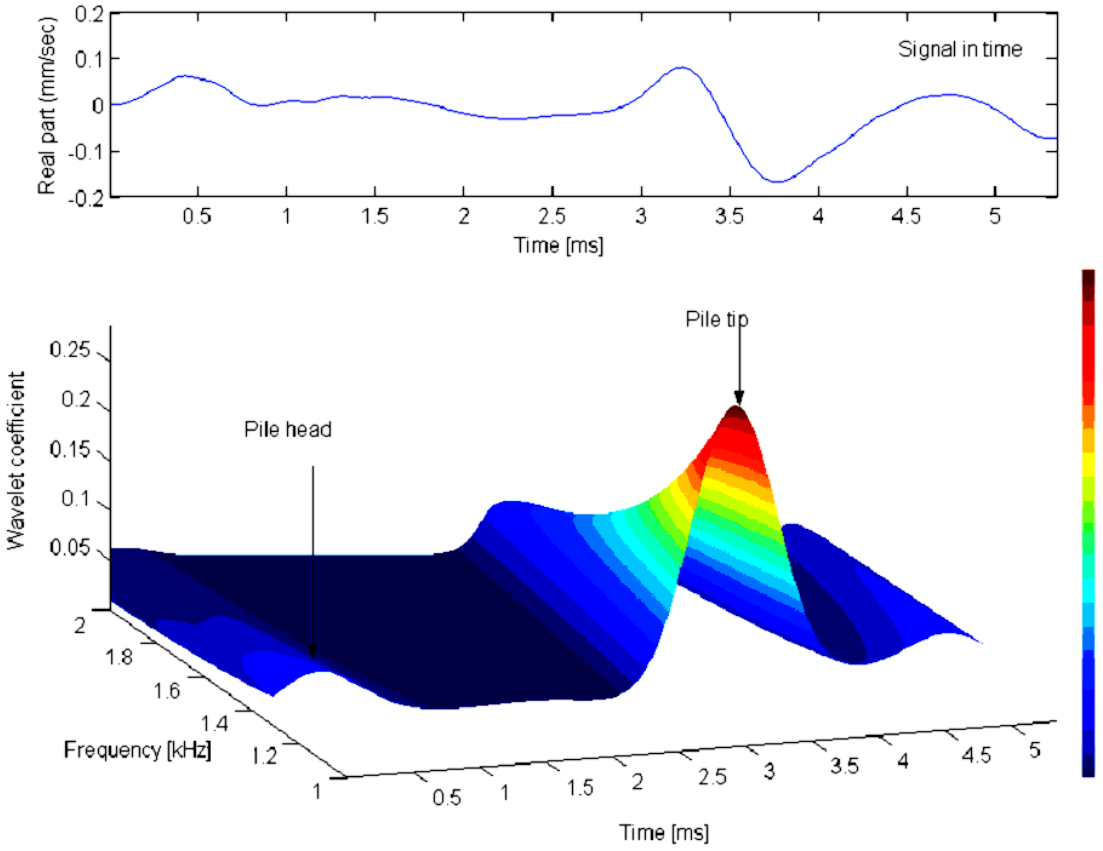

Fig. 6 CWT of PC intact pile

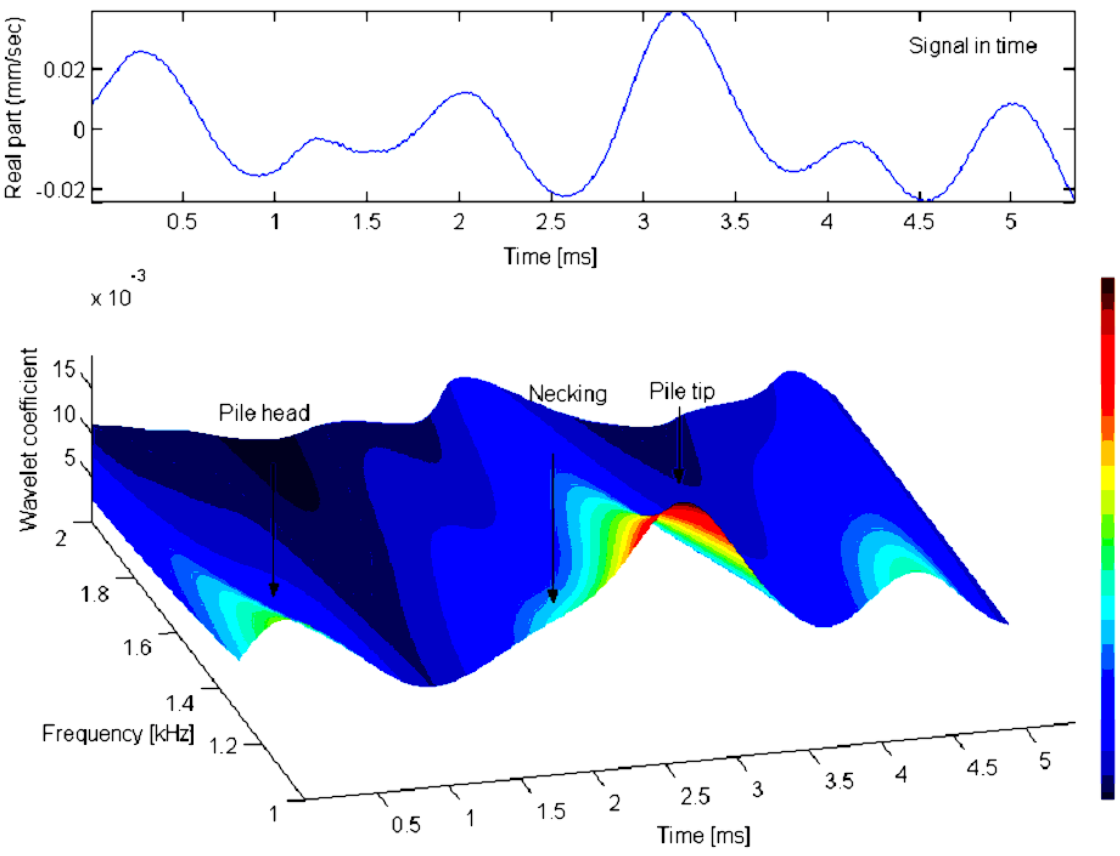

Fig. 7 CWT of the PC pile with necking

The test results of the total of 56 piles are shown in Table 1. The Table shows the pile length evaluated using SE test with WTM. The error of each pile compared with designed length of 53 m is also in these Tables. The test results for the 56 piles found a mean length of 52.09 m with a standard deviation of 2.49 m. The differences range from zero to 10% or so. The summary of the test results is listed in Table 2. As shown in the table, for more than 62.5% of test piles, the error is less than ±5 percent. The question is why do the errors exist? There are two reasons that may create the errors. First, the wave velocity was assumed to be 4,000 m/sec when calculating the length of the pile. Second, the length of pile constructed may differ from designed length (53 m). Both reasons may cause the errors in evaluation of the true pile length. In this study, the wave velocity of each pile was not measured. To measure correctly the pile length, it needs to consider using other NDT method, *e.g.*, ultra-seismic method or parallel seismic test, to measure the wave velocity of pile. In addition, no obvious defects were found in these piles.

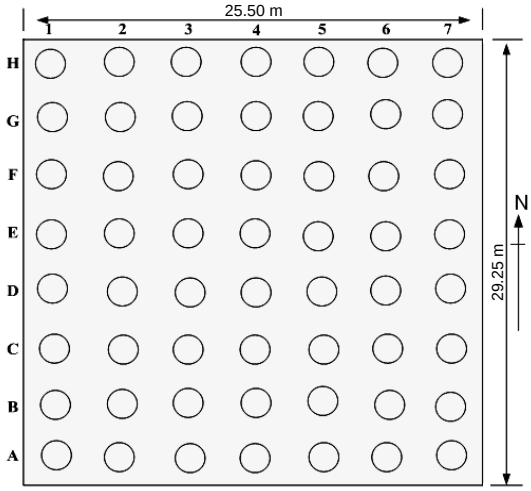

Fig. 8 Layout of piles in the test site

Fig. 9 Picture of test site

Fig. 10 Drilled shafts at the test site

Fig. 11 Sonic echo testing

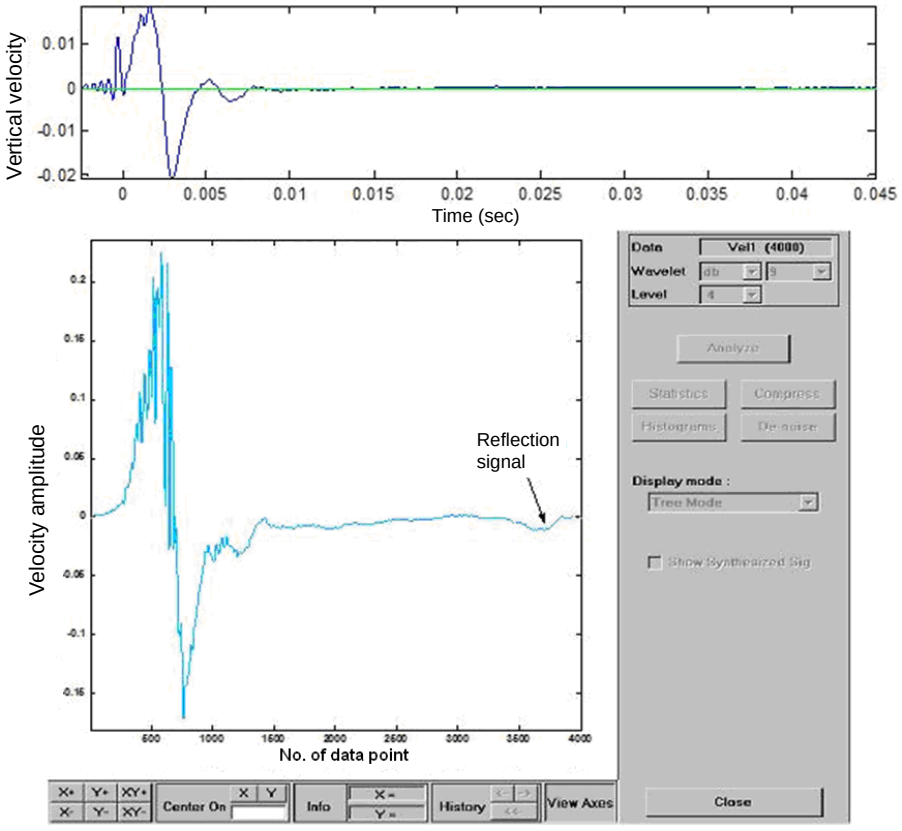

Fig. 12 Typical result of sonic echo test of drilled shaft

Table 1 Pile length evaluated and errors comparing with designed length of 53 meters

Pile no.		Pile length evaluated (m)	Error (%)	Pile no.		Pile length evaluated (m)	Error (%)
A	1	53.62	1.2	E	1	48	–9.4
	2	59.99	7.5		2	50.52	–4.7
	3	50.13	–5.4		3	53.01	0
	4	49.8	–5.7		4	53.01	0
	5	50.9	–4		5	53.6	1.1
	6	49.42	–6.7		6	53.21	0.4
	7	54.22	2.3		7	50.06	–5.5
B	1	52.15	–1.6	F	1	49	–7.5
	2	49	–7.5		2	50	–5.6
	3	50.37	–4.9		3	56.32	6.3
	4	54.44	2.7		4	52.54	–0.9
	5	52.35	–1.2		5	52.6	–0.8
	6	50	–5.6		6	52.12	–1.7
	7	51.42	–3		7	52.73	–0.5
C	1	50.48	–4.8	G	1	49.64	–6.3
	2	49.35	–6.9		2	52.58	–0.8
	3	52.41	–1.1		3	51.7	–2.5
	4	55.4	4.5		4	53.62	1.2
	5	55.86	5.4		5	51.16	–3.5
	6	53.12	0.2		6	54.53	2.9
	7	45	–15		7	54.03	1.9
D	1	49.64	–6.3	H	1	53.01	0
	2	50.2	–5.3		2	50.05	–5.6
	3	51.09	–6.6		3	50.81	–4.1
	4	52.54	–0.9		4	56.73	7
	5	56.6	6.7		5	51.93	–2
	6	51.86	–2.1		6	52.48	–1
	7	54.29	2.4		7	52.54	–0.9

Table 2 Summary of test results

Error range	–10% ~ –15%	–5% ~ –10%	–5% ~ 0	0 ~ +5%	+5% ~ +10%
No. of piles	1	15	21	14	5
Percentage (%)	1.8	26.8	37.5	25.0	8.9

6. CONCLUSIONS

Wavelet analysis is a mathematical technique and signal process tool which allows the signal to be viewed in the wavelet time-frequency domain. This is a new approach to analyze the signal for the SE method. The main goal of this paper is to discuss the feasibility of coupling the SE method and CWT in the time-frequency domain. The results show that such an approach may provide a more complete way of viewing the signal. The following conclusions can be drawn:

1. The wavelet analysis of the SE method can reveal detailed characteristics, including the pile tip and defects visualized in the time-frequency domain of CWT. Hence, SE testing results can be judged more easily, effectively and reliably than with traditional methods.
2. In the past, the time and frequency relationships of signals could be presented and interpreted by the traditional FT method. The SE testing signal can now be displayed in the time-frequency domain simultaneously by using CWT. The frequency change can be localized at any time in the whole signal.
3. The feasibility of coupling CWT and SE methods to interpret and identify the pile integrity visualize, easily and quickly is proven, even for long drilled shafts.

REFERENCES

Addison, P. S., Sibbald, A., and Watson, J. N. (1997). "Wavelet analysis: A mathematical microscope with civil engineering applications." *Insight*, **39**(7), 493–497.

Addison, P. S. and Watson, J. N. (1997). "Wavelet analysis for low-strain integrity testing of foundation piles." *Proc. 5th Intl. Conf. On Inspection, Appraisal, Repairs, Maintenance of Buildings and Structures*, Singapore, 15–16.

Addison, P. S., Watson, J. N., and Feng, T. (2001). "Low-oscillation complex wavelets." *Journal of Sound and Vibration*, **254**(4), 733–762.

Daubechies, I. (1992). *Ten Lectures on Wavelets, Society for Industrial and Applied Mathematics*, Philadelphia, Pennsylvania, 129–131.

Gabor, D. (1946). "Theory of communication." *J. IEEE*, London, 429–457.

Hartung, M., Meier, K., and Rodatz, W. (1992). "Integrity testing on model pile." *Proc., 4th Int. Conf. on the Application of Stress-Wave Theory to Piles*, 265–271.

Lin, S. S., Wang, K. J., Hsieh, H. S., Chang, Y. H., and Huang, C. H. (2007). "Field testing of axially loaded drilled shafts in clay/gravel layer." *Journal of GeoEngineering*, **2**(3), 123–128.

MathWorks Inc. (1996). *Wavelet Toolbox for Use with Matlab User's Guide*, 1–99.

Morlet, J. and Grossmann, A. (1984). "Decomposition of hardy functions into square integrable wavelets of constant shape." *J. Math*, **15**, 723–736.

Ni, S. H. and Lo, K. F. (2006). "Pile integrity testing signal analyses with one dimensional continuous wavelet transform." *Proceedings of the 16th International Offshore and Polar Engineering Conference*, CD-ROM, San Francisco, USA.

Ni, S. H., Lo, K. F., and Huang, Y. H. (2006). "The application of wavelet transform to sonic echo testing of pile." *Proceedings of 2006 Cross-Strait Workshop on Engineering Mechanics*, Sept., Taipei, Taiwan.

Ni, S. H., Charng, J. J., and Lo, K. F. (2007). "Nondestructive evaluation of in-isolation pile shaft integrity by Wigner-Ville distribution." *Journal of Mechanics*, **23**(1), 15–21.

Ni, S. H., Lehmann, L., Lo, K. F., and Huang, Y. H. (2007). "Time-frequency analyses of pile integrity testing using wavelet transform." *Computers and Geotechnics*, **35**(4), 600–607.

Olson, L. D. and Wright, C. C. (1989). "Non-destructive testing of deep foundations with sonic methods." *Proc. Found. Engineering Congress: Current Principles and Practice*, ASCE, **2**, Reston, Va., 1173–1183.

Seidel, J. P. (2000). "Presentation of low strain integrity testing in the time-frequency domain." *Proc. 6th Int. Conference on the Application of Stress-Wave Theory to Piles*, Rotterdam, 193–200.

Watson, J. N. and Addison P. S. (2002). "Spectral-temporal filtering of NDT data using wavelet transform modulus maxima." *Mechanics Research Communications*, **29**(2-3), 99–106.